# THE INFLUENCE OF HYDROTHERMAL TREATMENT ON THE STRUCTURE AND $CO_2$ UPTAKE CAPACITY OF A CaO SORBENT DERIVED FROM CRAB SHELL

D. BACIU[*], T. STERIOTIS, G. CHARALAMBOPOULOU, A. STUBOS
*National Center for Scientific Research "Demokritos", 15310 Agia Paraskevi*
*Attikis, Athens, Greece,*

A mesoporous CaO-based sorbent was successfully synthesized by a new hydrothermal method based on the treatment of CaO particles derived from crab shell. Multi-cyclic carbonation/decarbonation experiments showed that the new mesoporous CaO-based sorbent possesses a higher $CO_2$ adsorption capacity (8.01 mmol $CO_2$/g sorbent) compared with the CaO particles obtained after the calcination of crab shell at 900 $^0$ C, where a $CO_2$ adsorption capacity of 3.26 mmol $CO_2$/g sorbent was observed for the first carbonation/decarbonation cycle. In addition, the CaO-based sample sythesized by the hydrothermal treatment and calcination of the CaO-crab shell derived particles possesses a mesoporous structure and a higher surface area (33.63 $m^2$/g).

(Received December 21, 2015; Accepted February 26, 2016)

*Keywords:* CaO-based sorbents, $CO_2$ uptake capacity, SEM

## 1. Introduction

It is generally accepted that the excessive use of fossil fuels has led to global warming and anthropogenic climate change due to the increase of greenhouse gas emissions and mainly of $CO_2$. A promising concept for $CO_2$ separation from combustion flue gases is Carbonate Looping [1]. Calcium Looping Process (CLP) for $CO_2$ removal, which is based on the reversible reaction: $CaO(s) + CO_2(g) \leftrightarrow CaCO_3(s)$, exhibits a promising prospect. Calcium oxide is generally obtained from naturally occurring limestone, but it suffers the problem of losing-capacity during a long series of carbonation/calcination cycles, which is attributed to the sintering of the sorbent [2]. Promising methods to increase durability of sorption capacity of sorbents involve modifying the textural properties of CaO-based $CO_2$ sorbent, thermal pretreatment of the sorbent, sorbent doping with additives (e.g., MgO and $Ca_{12}Al_{14}O_{33}$), steam hydration treatment, and change of the precursors [3].

This work involves the preparation and characterization of two new CaO-based sorbents as well as the investigation of their reactivity towards $CO_2$. A new hydrothermal method was used to treat CaO particles in the presence of cetyltrimethylammonium bromide (CTAB) and polyethylene glycol (PEG) co-surfactants, followed by drying and calcination. Hydrothermal treatment was conducted at 220$^0$C for 4h and its influence on structure and $CO_2$ uptake capacity of the obtained CaO-based sorbent was investigated. The pertinent structural, morphological and textural properties were investigated by SEM, XRD, TGA and $N_2$ adsorption at 77K. The carbonation/decarbonation cycling performance of the materials (powder form) was measured in the course of up to 4 cycles by thermogravimetric analysis.

## 2. Experimental

Mesoporous CaO-based sorbents were synthesized by a hydrothermal method in the presence of cetyltrimethylammonium bromide (CTAB) and polyethylene glycol (PEG) as cationic surfactant and non-ionic co-surfactant, respectively. Briefly, under continuously stirring, 2 g of

---

[*] Corresponding author: dianabaciuro@yahoo.com

irregularly morphological CaO powders from crab shell (crab shell calcined at 900 $^0$C/ 4 h), 0.7 g CTAB (Sigma) and 0.23 g NaOH (Mallinckrodt) were added to 60 mL of deionized water containing 2.5 g of PEG (Aldrich, average Mn (10.000)). After being stirred for 1 h, the mixed solution was transferred to Teflon-lined stainless steel autoclaves for hydrothermal treatment at 220 $^0$C for 48 h. The products were collected by filtration and washed by ddH$_2$O and ethanol several times. Then the collected powders were dried in an oven at 80 °C for 48 h and calcined in air at a heating rate of 9 $^0$C / min from RT to 550 $^0$C and kept at this temperature for 3 h, thus generating the mesoporous CaO-based sample.

The powder X-ray diffraction (PXRD) patterns of the samples were recorded on a Rigaku R-AXIS IV Imaging Plate Detector mounted on a Rigaku RU-H3R Rotating Copper Anode X-ray Generator ($\lambda$ = 1.54 Å).

SEM images of the developed materials were obtained using a Jeol JSM 7401F Field Emission Scanning Electron Microscope (SEM). The materials were subjected to gold coating prior to SEM imaging.

The nitrogen adsorption/desorption isotherms at 77 K were measured in an automated volumetric system (AUTOSORB-1, Quantachrome Instruments). Prior to measurement, the samples were outgassed at 250 °C for 12 h.

The infrared spectra (IR) spectra were obtained using a Thermo Scientific Nicolet 6700 FTIR equipped with a N$_2$ purging system and a LN2-cooled wide range Mercuric Cadmium Telluride detector.

## 3. Results and Discussion

Fig. 1 (a-f) shows SEM images of CaO particles derived from crab shell (Sample_CR900) and of mesoporous CaO-based sorbent (Sample_CR550).

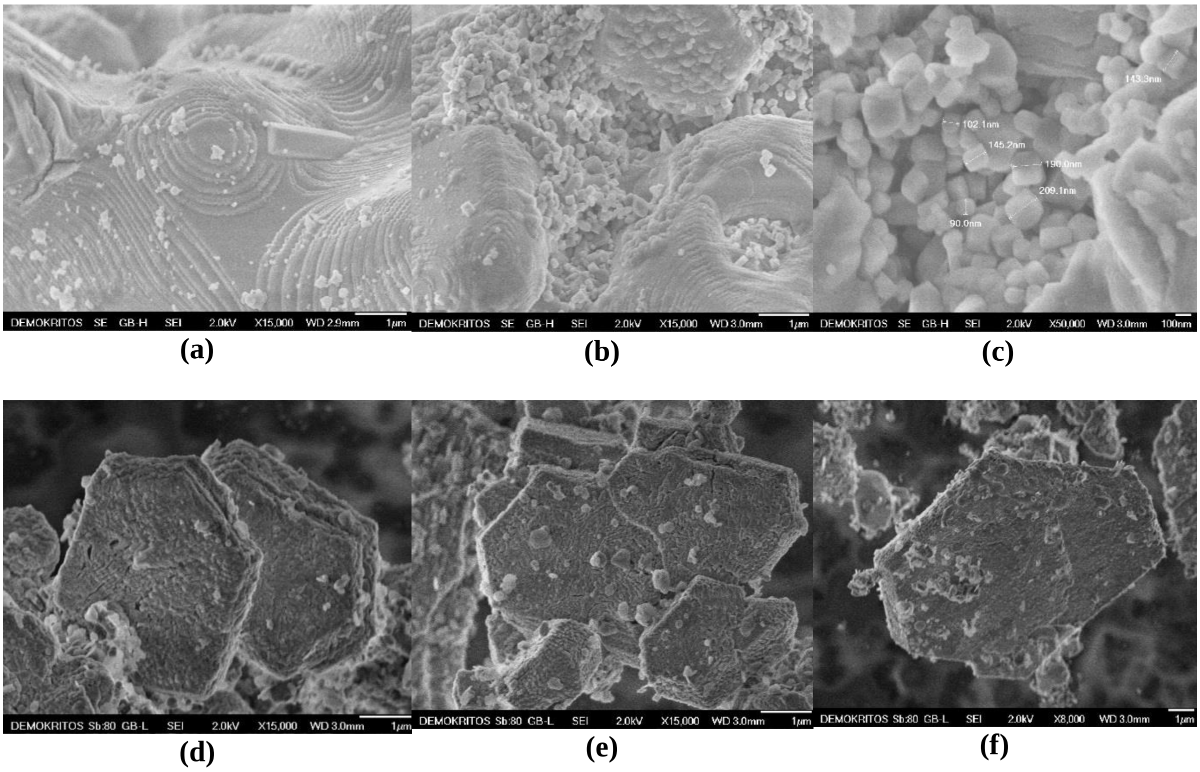

*Fig. 1. SEM images of the CaO-based sorbents prepared after (a, b, c) calcination of crab shell at 900 °C (Sample_ CR900) and ( d, e, f) hydrothermal treatment at 220 °C for 4 h followed by drying and calcination at 550 $^0$C for 3h (Sample_CR550).*

According to literature, highly ordered superstructures with a well-defined external morphology could be obtained under hydrothermal conditions due to the presence of CTAB [4] and PEG [5] as co-surfactants. Initially CaO powders hydrated to $Ca(OH)_2$ nanoparticles, which then were reacted with PEG and aggregated into hexagonal entities. After thermal treatment in air at 550 $^0$C for 3 h, particles with hexagonal prism morphologies were formed. The influence of hydrothermal treatment on the morphology of CaO particles derived from the crab shell is clearly observed. Thus, the Sample_CR900 (Fig. 1(b, c)) contains agglomerated cubic particles, while the Sample_CR550 (Fig.1 (d, e, f)) displayed only particles with hexagonal prism morphology.

The $N_2$ adsorption/desorption isotherms at 77 K of the as-prepared samples are presented in Fig. 3a. The analysis of the respective data showed a BET specific surface area of 6.11 $m^2/g$ (Sample_CR900) and 33.63 $m^2/g$ (Sample_CR550), respectively. The Sample_CR550 exhibits a typical type IV isotherm with hysteresis, characteristic for mesoporous materials. It can be seen that the surface area of the as-prepared samples was highly dependent upon the fabrication procedure adopted.

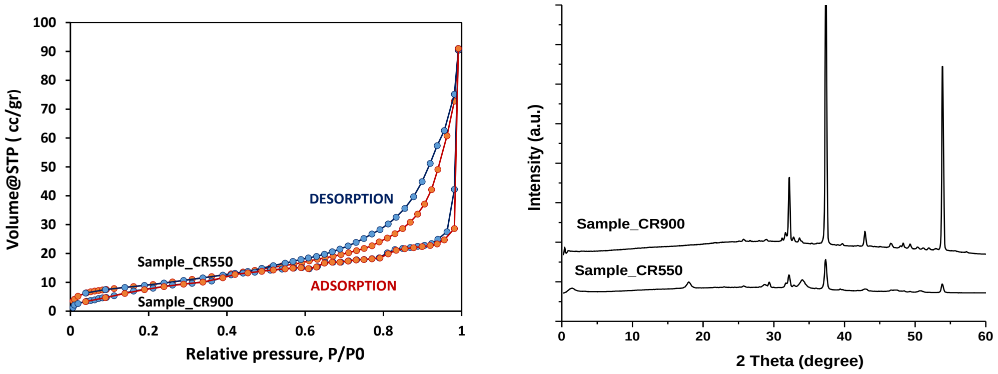

(a) (b)

*Fig. 3: (a) $N_2$ adsorption/desorption isotherms of the (a) CR900 and (b) CR550 samples; (b) X-ray diffraction patterns of the prepared CaO-based sorbents.*

According to XRD pattern depicted in Fig. 3b (Sample_CR900), the calcined crab shell powder shows peaks at $2\theta = 32.2°$, 37.35°, 43.97°, 50.4° and 53.9°, which belong to the calcium oxide (CaO) (CaO, JCPDS Card No. 00-002-1088) [6, 7]. Similar peaks can be observed in the XRD pattern of the CaO-based sorbent hydrothermally prepared at 220 $^0$C and calcined at 550 $^0$C (Fig 3 (Sample_CR550)). In addition, Sample _550 shows peaks which belong to the portlandite ($Ca(OH)_2$), and calcium carbonate ($CaCO_3$). Specifically, the peaks at $2\theta$ values of around 18°, 28°, 34° and 47°, correspond to portlandite phase (Portlandite, JCPDS card No. 00-002-0968), which indicated the hydroxylation reaction occurred in between water and CaO phases [8, 9]. The peaks at $2\theta$ values of around 34°, 39°, 43° and 48°, respectively, correspond to calcite ($CaCO_3$) phase (JCPDS Card no. 72-1652) [10].

Multi-cyclic carbonation/decarbonation performance of the materials (powder form) was measured in the course of up to 4 cycles in a thermogravimetric analysis instrument (SETARAM SETSYS Evolution 18 Analyzer). Specifically, the TGA measurements were performed on ~10 mg of each sample in an $Al_2O_3$ crucible. The carbonation reaction took place at 600$^o$C under 100% $CO_2$ atmosphere, while the decarbonation reaction was conducted at 800$^o$C under 100% Ar flow. The results of $CO_2$ capture performance of the materials studied are comparatively shown in Fig. 4 and Table 1.

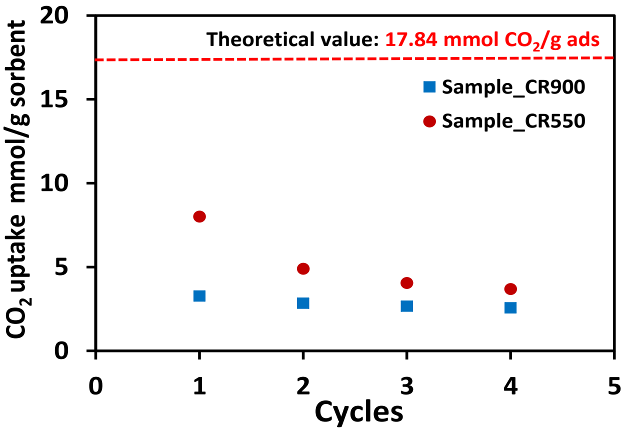

*Fig. 4. Evaluation of the as-prepared CaO-based samples up to 4 carbonation-decarbonation cycles.*

*Table 1. $CO_2$ uptake capacity and maximum efficiency (%) of CaO-based sorbents*

| Sample | BET surface area ($m^2$/g) | $CO_2$ adsorption capacity (mmol $CO_2$/g sorbent) | | | | Max. Efficiency (%)* |
|---|---|---|---|---|---|---|
| | | 1st cycle | 2nd cycle | 3rd cycle | 4th cycle | |
| Sample_CR900 | 6.11 | 3.26 | 2.84 | 2.67 | 2.57 | 18 |
| Sample_CR550 | 33.63 | 8 | 4.9 | 4.05 | 3.69 | 45 |

*Max. Efficiency = (max. measured capture capacity)/(theoretical capacity of pure CaO) %
Theoretical capacity of pure CaO = 17.84 mmol/g CaO

According to Fig. 4 and Table. 1, the mesoporous CaO-based sorbent synthesized by the hydrothermal treatment exhibits a higher $CO_2$ adsorption capacity (8.01 mmol $CO_2$/g sorbent) compared with the CaO perticles obtained after the calcination of crab shell at 900 $^0$ C, where a $CO_2$ adsorption capacity of 3.26 mmol $CO_2$/g sorbent was observed for the first carbonation/decarbonation cycle. This is in agreement with previous studies which showed that the sorption capacity of $CO_2$-sorbent materials depends on the surface area of the material [11].

## 4. Conclusions

In this work a new mesoporous CaO-based sorbent was successfully synthesized by the hydrothermal treatment of CaO particles derived from crab shell in the presence of CTAB and PEG co-surfactants, followed by drying and calcination. The use of the hydrothermal treatment proved to be beneficial, resulting in the calcium oxide particles with higher surface area and $CO_2$ uptake capacity. Furthermore, morphological changes of the samples were observed.

## Acknowledgements

D. Baciu gratefully acknowledges the Greek General Secretariat for Research & Technology for partially funding of this work through the NESTOR Project (Bilateral RTD Greece-Germany Cooperation 2013-2015; Project code 2051).

## References

[1] A. Antzara, E. Heracleous, A. A. Lemonidou, Applied Energy **156**, 331 (2015).
[2] H. Yingchao, L.Wenqiang, S. Jian, Y. Xinwei, Z. Yang, X. Minghou, Chemical Engineering

Journal **273**, 333 (2015).
[3] L. Peiqiang, W. Sufang, Fuel **143**, 9 (2015).
[4] C. J. Murphy, Advanced Materials **14**(1), 80 (2002).
[5] Y. Zusing, H. L. Zong, T. Chih-Yuan and C. Huan-Tsung, Nanonotechnology **18** (25), 255606 2007.
[6] L. M. Correia, M. A. Saboya, N. S. Campelo, J. A. Cecilia, E. R. Castellon, Jr C. L. Cavalcante, R.S. Vieira, Bioresource Technology **151**, 207 (2014).
[7] N. Asikin-Mijan, Y.H. Taufiq-Yap, H.V. Lee, Chemical Engineering Journal **262**, 1043 (2015).
[8] A. Kawashima, K. Matsubara, K. Honda, Bioresour. Technol. **100**, 696 (2009).
[9] Y. C. Sharma, B. Singh, S.N. Upadhyay, Fuel **87**, 2355 (2008).
[10] Y. Chengli, X. Anjian, S.Yuhua, Z. Jinmiao, L. Tengjiao, J. Chil. Chem. Soc., **58**, Nº 4 (2013).
[11] S. Hu, Y.Wang, H. Han, Biomass Bioenergy **35**, 3627 (2011).